BBA - Molecular Basis of Disease 1865 (2019) 2694–2705

Contents lists available at ScienceDirect

BBA - Molecular Basis of Disease

journal homepage: www.elsevier.com/locate/bbadis

Knocking out *lca5* in zebrafish causes cone-rod dystrophy due to impaired outer segment protein trafficking

Zhen Qu[a,1], Tinsae Assefa Yimer[a,1], Shanglun Xie[a,1], Fulton Wong[b], Shanshan Yu[a], Xiliang Liu[a], Shanshan Han[a], Juanjuan Ma[a], Zhaojing Lu[a], Xuebin Hu[a], Yayun Qin[a], Yuwen Huang[a], Yuexia Lv[a], Jingzhen Li[a], Zhaohui Tang[a], Fei Liu[a,*], Mugen Liu[a,**]

[a] *Key Laboratory of Molecular Biophysics of Ministry of Education, College of Life Science and Technology, Huazhong University of Science and Technology, Wuhan, Hubei 430074, PR China*

[b] *Department of Ophthalmology, Duke University School of Medicine, Durham, NC 27710, USA*

ARTICLE INFO

Keywords:
LCA5
CRISPR/Cas9
Zebrafish
Photoreceptor degeneration
Ift88

ABSTRACT

Leber congenital amaurosis (LCA) is the most serious form of inherited retinal dystrophy that leads to blindness or severe visual impairment within a few months after birth. Approximately 1–2% of the reported cases are caused by mutations in the *LCA5* gene. This gene encodes a ciliary protein called LCA5 that is localized to the connecting cilium of photoreceptors. The retinal phenotypes caused by *LCA5* mutations and the underlying pathological mechanisms are still not well understood. In this study, we knocked out the *lca5* gene in zebrafish using CRISPR/Cas9 technology. An early onset visual defect is detected by the ERG in 7 dpf *lca5*$^{-/-}$ zebrafish. Histological analysis by HE staining and immunofluorescence reveal progressive degeneration of rod and cone photoreceptors, with a pattern that cones are more severely affected than rods. In addition, ultrastructural analysis by transmission electron microscopy shows disordered and broken membrane discs in rods' and cones' outer segments, respectively. In our *lca5*$^{-/-}$ zebrafish, the red-cone opsin and cone α-transducin are selectively mislocalized to the inner segment and synaptic terminal. Moreover, we found that Ift88, a key component of the intraflagellar transport complex, is retained in the outer segments. These data suggest that the intraflagellar transport complex-mediated outer segment protein trafficking might be impaired due to *lca5* deletion, which finally leads to a type of retinal degeneration mimicking the phenotype of cone-rod dystrophy in human. Our work provides a novel animal model to study the physiological function of *LCA5* and develop potential treatments of LCA.

1. Introduction

Leber congenital amaurosis (LCA) is the earliest and most severe form of inherited retinal dystrophy causing blindness or severe visual impairment in the first few months after birth [1,2]. The manifestations of LCA in patients are highly variable, usually including severe and early visual loss, sensory nystagmus, amaurotic pupils, and absent electrical signals on electroretinogram (ERG) [3]. Although rare dominant cases have been reported, LCA is inherited most frequently as an autosomal-recessive trait [4–6]. Twenty-five genes have been reported responsible for LCA (https://sph.uth.edu/retnet/home.htm). These genes encode proteins with a wide variety of retinal functions, including phototransduction, visual cycle, photoreceptor development, guanine synthesis and intra-photoreceptor ciliary transport processes [5,7–11]. Mutations in Leber congenital amaurosis 5 (*LCA5*, OMIM *611408) gene accounts for about 1%–2% of LCA [1].

The *LCA5* locus was initially mapped to chromosome 6p14.1 by linkage analysis in two inbred families of the Old Order River Brethren and the Pakistani family [12,13]. Subsequently, the causative gene, *LCA5*, was identified by den Hollander in 2007 [14]. *LCA5* consists of eight exons, seven of which encode LCA5, a 697-amino acid protein that contains two coiled-coil domains [14]. To date, 36 different mutations in *LCA5* have been reported worldwide [14–23]. These mutations are evenly distributed and there seems to be no obvious mutation

* Correspondence to: F. Liu, Key Laboratory of Molecular Biophysics of Ministry of Education, Center for Human Genome Research, Huazhong University of Science and Technology, Wuhan, Hubei 430074, PR China.

** Corresponding author.

E-mail addresses: liufei05@hust.edu.cn (F. Liu), lium@mail.hust.edu.cn (M. Liu).

[1] These authors contributed equally to this work.

https://doi.org/10.1016/j.bbadis.2019.07.009
Received 27 March 2019; Received in revised form 6 July 2019; Accepted 22 July 2019
Available online 23 July 2019

hotspots. Moreover, twenty-nine of these mutations are nonsense, frameshift or splice site mutations, which are predicted to introduce a premature termination codons and result in loss of function of LCA5 protein. In addition to LCA, mutations of *LCA5* also cause early-onset retinal dystrophy (EORD), retinitis pigmentosa (RP) and cone dystrophy (CD) rarely [20,21].

LCA5 is an evolutionary conserved ciliary protein that localizes to the connecting cilia of photoreceptors and the primary cilia of cultured mammalian cells [14,24]. Although *LCA5* is widely expressed throughout development, the disease phenotype is restricted to the eye [14]. LCA5 physically interacts with OFD1, which may be a potential mechanism of retinal degeneration in patients with Joubert syndrome caused by OFD1 mutations [25]. In addition, LCA5, USH2A isoform B and Nlp isoform B co-localize at the centrosomes in ARPE-19 cells and at the basal bodies of the photoreceptor-connecting cilia in rat retina [26]. Furthermore, affinity proteomics and yeast-two-hybrid approach have identified many possible LCA5 interacting proteins involved in protein transport, such as IFT complex B, IFT complex B associated proteins, IFT complex A and motor proteins [14,24]. Inactivation of *Lca5* in mouse results in delayed development of photoreceptor outer segments and disordered outer segment structure, which eventually leads to rapid degeneration of the outer and inner segments of photoreceptor cells. Although the structure of connecting-cilia and the basal body appears to be normal, the rod and cone opsins mislocate to the photoreceptor inner segments and outer nuclear layer. Arrestin and transducin also partially mislocalize in response to light [24]. These studies suggest that LCA5 may play an important role in selective protein transport of photoreceptor cilia. However, the specific mechanism of how *LCA5* mutations cause retinal degeneration is still not fully understood.

Zebrafish have a retinal structure similar to that of humans, and the ratio of rods to cones is very similar to that of humans. These factors determine that zebrafish may be a more suitable animal model for investigating the pathogenic mechanisms of human retinal diseases [27,28]. In zebrafish, *lca5* contains 8 exons encoding a protein of 754 amino acids, which is conserved between human and zebrafish. Until now, there is no report about the gene function of *lca5* or the retinal phenotypes after *lca5* deletion in zebrafish.

In this study, we constructed the *lca5* knockout zebrafish model by CRISPR/Cas9 technology. We identified a *lca5* mutant zebrafish line with a c.18_21delTAAT (p.Asn7Argfs*17) mutation, which is predicted to cause premature termination of translation and result in a truncated protein with no function. The retinal phenotypes and the underlying pathological mechanisms were further investigated.

2. Materials and methods

2.1. Animals

The study was approved by the Ethics Committee of Huazhong University of Science and Technology. Zebrafish AB line were maintained as described [29,30]. Zebrafish were raised in 28 °C constant temperature circulating water system with a daily cycle of 14 h of light and 10 h of dark. Zebrafish are sexually mature at 3 months of age and can breed offspring. The male and female zebrafish used for reproduction are mated every 7 days and the eggs are collected and transferred to E3 medium.

2.2. Generating lca5 mutant by CRISPR/Cas9 technology

The CRISPR/Cas9 system was purchased from the China Zebrafish Resource Center (CZRC). CRISPR/Cas9 target sites were designed using the online tool at: http://chopchop.cbu.uib.no/. The target sequences are 5′ GGACTTGCATGAAGATAATC 3′. The target gRNA and capped Cas9 mRNA were synthesized using TranscriptAid T7 High Yield Transcription Kit (Thermo Scientific) and mMESSAGE mMACHINE mRNA transcription synthesis kit (Ambion). 8 nl of Cas9 mRNA (300 ng/ul) and gRNA (20 ng/ul) were co-injected into one-or two-cell stage wild type embryos. After 50 h of injection, 10–15 embryos were collected from F0 embryos, whose genomes were extracted to evaluate CRISPR/Cas9 system-mediated target efficiency. A 337 bp DNA fragment spanning the *lca5* target site was amplified by PCR (forward primer: 5′-CAGCTTGAGTGTTGAGTGT-3′; reverse primer: 5′-GCTCTGT GCATGATCCC-3′) and sequenced. The validated F0 zebrafish were raised to adult and used to produce F1 generations by crossing them to wild-type zebrafish. The F1 zebrafish were further subjected to DNA sequencing to identify the exact mutations. Males and females carrying the same mutation mated with each other to make homozygotes. F2 zebrafish were identified using the same method described above.

2.3. Electroretinography

Zebrafish (7 dpf) were placed in the dark for at least 30 min, then anesthetized with Esmeron (0.8 mg/mL) for 1–2 min, and placed on the wet tissue corresponding to the reference electrode. The tip of the glass microelectrode was placed in the center of the cornea (contact with the cornea gently) of the zebrafish. The zebrafish was again adapted to the complete dark environment for at least 2 min. Turn on Clampex 10.4 to start recording the signal. Zebrafish eye was illuminated by light for 1 s, and the interval between the two exposures is about 10 s.

2.4. Hematoxylin and eosin (H&E) staining

Zebrafish eyeball were dissected and fixed at 4 °C overnight in 4% paraformaldehyde, and dehydrated in 30% sucrose. For cryosections, adult or embryo eyecups were embedded in O.C.T. Cryosections were hematoxylin and eosin stained under standard conditions. The sections after HE staining were observed and photographed under the optical microscope BX53.

2.5. Immunofluorescence

Immunofluorescence was performed as described [31]. After the frozen slices were taken out of the refrigerator, they were balanced at room temperature for 20 min. Slides containing sections were incubated with PDT (PBS/1%DMSO/0.1%Triton) for 10 min and blocked with 10% goat serum in PBDT (PDT/1%BSA/10%goat serum). Primary antibodies were diluted to the indicated concentration (shown in Supplementary Table S1) with 2% goat serum in PBDT and added onto the slides, which were incubated overnight at 4 °C. Primary antibody was removed and the slice was rinsed three times in the PDT for 10 min each time. Second antibody (Alexa-Fluor 488-nm or 594-nm secondary antibody) was added to the slice and incubated at 37 °C in dark for 1 h. DAPI staining was followed, and DAPI was diluted to the final concentration of 0.5 μg/mL with PBS, and then the section was stained for 5 min. Next, the section was rinsed three times in PBS for 15 min each time. The last step, section was mounted with a glycerol-based liquid mountant under coverslips. Fluorescence images were captured using a confocal laser-scanning microscope (FluoView™ FV1000 confocal microscope, Olympus Imaging).

2.6. Transmission electron microscopy

TEM was performed according to previous literatures [32]. Zebrafish eyes were isolated and their lenses removed, and the eyes fixed in 2.5% glutaraldehyde in 0.1 M PBS overnight at 4 °C. After washing

three times, the samples were added to 1% osmium tetroxide and fixed at room temperature for 2 h. Then the samples were gradient dehydrated with ethanol and incubated in acetone at room temperature for 20 min. After propylene oxide treatment and embedding in epoxy resin, Reichert-Jung ultramicrotome was used to produce ultrathin slices. Specimens stained with uranyl acetate and lead citrate were observed and photographed using transmission electron microscopy (HT7700, Hitachi).

2.7. Western blot

Fresh zebrafish eyeball were placed on the ice, and appropriate amount of RIPA lysate was added for digestion. Tissue samples were broken by ultrasound to allow cell to full lyse. Then the samples were added to a 1/5 volume 5 X loading buffer, boiled for 10 min, and immediately soaked in ice for 2 min. Protein samples were separated by SDS-PAGE gel and immunoblotting onto NC membranes. Membranes were then blocked in 5% nonfat milk solution in TBST for 1 h at room temperature followed by incubation with primary antibody (shown in Supplementary Material, Table S1) at 4 °C overnight. The membranes were washed three times in TBST for 8 min each and incubated in HRP-conjugated secondary antibodies (1:20,000; Thermo) for 2 h at room temperature. The membranes were washed three times with TBST for 8 min each time. Finally, the protein was quantitatively analyzed by ChemiDoc XRS + system (Bio-Rad).

2.8. Statistical analyses

Experiments were repeated at least three times. GraphPad Prism 6.0 was used for statistical analysis. Two-tailed Student's *t*-test was used for determining significance.

2.9. Key resources table

Resource	Source	Identifier
Chemical		
Acetone		
DAPI		
DMSO		
Eosin		
Epoxy		
Esmeron		
Ethanol		
Glutaraldehyde		
Glycerol		
Hematoxylin		
Hematoxylin		
Lead citrate		
Osmium tetroxide		
Propylene oxide		
Sucrose		
Uranyl acetate		
ProteinPeptide		
Acetylate a-Tubulin	**N/A**	**N/A**
Cas9		
CRISPR		
gnat1	**N/A**	**N/A**
gnat2	**N/A**	**N/A**
gnb3	**N/A**	**N/A**
grk1	**N/A**	**N/A**
gRNA		
HRP		
Ift88	**N/A**	**N/A**
opn1lw1	**N/A**	**N/A**
opn1mw1	**N/A**	**N/A**
opn1sw1	**N/A**	**N/A**
opn1sw2	**N/A**	**N/A**
rhodopsin	**N/A**	**N/A**
XRS		

3. Results

3.1. Generation of lca5 knockout zebrafish using CRISPR/Cas9 technology

LCA5 protein sequences of human, mouse, rat, chicken, xenopus, and zebrafish were downloaded from NCBI. Sequence alignment across different species was performed by the COBALT tool (https://www.ncbi.nlm.nih.gov/tools/cobalt/) [33] using the default parameters. The identical and positive amino acid residues were displayed in red and blue respectively, with the option of "conservation setting" set to "identity" (Supplementary Material, Fig.S1). The multiple alignment result showed that Lca5 is moderately conserved from zebrafish to human. About 19% (144/754) amino acid residues are identical and 78% (592/754) amino acid residues are positive across the six species. Moreover, in the N-terminal coiled-coil domain (157–351), zebrafish Lca5 contains more identical (40%, 79/195) and positive (100%, 195/195) amino acid residues (Fig. 1A, Supplementary Material, Fig.S1).

To generate the *lca5* knockout zebrafish by CRISPR/Cas9 technology, we downloaded the zebrafish *lca5* cDNA (XM_009297006) and genomic (NW_018395159) sequences from the NCBI database. Through online software, the target sites were designed at the second exon containing initial codon ATG (Fig. 1B). Meanwhile, we designed a pair of primers to amplify the region spanning the target site. The Cas9 mRNA and gRNA were co-injected into one-or two-cell stage wild type embryos. We identified a 4 bp deletion (c.18_21delTAAT, p.Asn7Argfs*17), named delTAAT, which resulted in premature termination at codon 17. Homozygous delTAAT zebrafish were identified and their offspring were validated by genomic DNA sequencing (Fig. 1C). To verify whether the mutant *lca5* mRNA is degraded by nonsense-mediated decay, we detected the mRNA levels of *lca5* in wt and *lca5* mutant zebrafish by qPCR. There is no significant decrease of *lca5* mRNA level in *lca5* knockout zebrafish compared with wild type at the age of 1 month (Fig. 1D). Furthermore, to distinguish the expression differences between the two transcripts of zebrafish *lca5*, two pairs of primers were designed, which could amplify the major transcript and both transcripts, respectively (Supplementary Material, Fig. S2A, Table S2). The expression level of both transcripts appears to be unaffected in *lca5* mutant zebrafish (Supplementary Material, Fig. S2B). To exclude the possibility that alternatively spliced transcript(s) might not be affected by this mutation, we amplified a fragment containing the mutation site using cDNA as template, and sequenced the fragment, which showed c.18_21TAAT is deleted in *lca5* mRNA in the *lca5* mutants (Supplementary Material, Fig. S3). These results demonstrated that the knockout of *lca5* in this study is effective.

3.2. Weakened visual function at an early stage in lca5 knockout zebrafish

In consideration of the fact that patients with *LCA5* mutations show early-onset severe visual impairment and significantly reduced or undetectable waves in ERG measurement, we also examined the visual function of the *lca5* knockout zebrafish at 7 dpf by ERG test. The vertebrate ERG originates in the outer retina and features three prominent waves, an initial negative a-wave reflecting photoreceptor activity, a large positive b-wave reflecting mainly ON-bipolar cell activity, and the d-wave reflecting postsynaptic activity involved in the OFF response [34]. Because of an overlap with b-wave, the a-wave almost completely disappears [35]. The scotopic b-wave amplitudes of *lca5* knockout zebrafish was calculated and decreased by 50% when compared with wild type controls (Fig. 2A, B), indicating that the ablation of *lca5* affects early visual function in zebrafish.

3.3. Progressive photoreceptor degeneration with a predominantly cone-affected pattern in lca5 knockout zebrafish

To investigate whether the retinal structure is affected by *lca5* knockout, we first performed histological analysis using wt and *lca5*

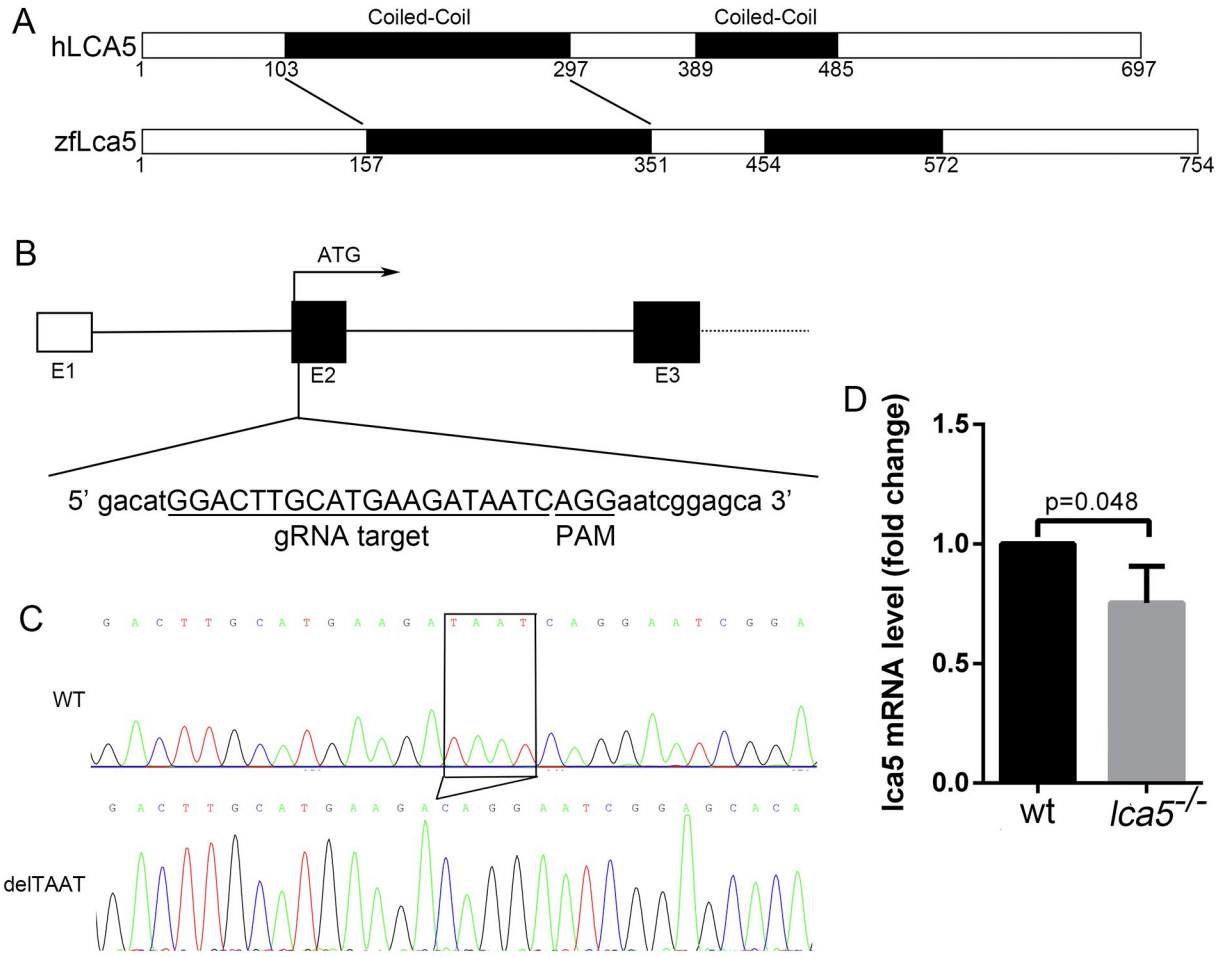

Fig. 1. Generation of *lca5* knockout zebrafish. (A) Conservative analysis of human and zebrafish Lca5. The amino terminal of LCA5 protein is more conserved in human and zebrafish. (B) The gRNA target sequence and the position of the corresponding *lca5* gene sequence are shown. E1-E3, exon1-exon3. (C) Sequencing validation of the c.18_21delTAAT mutation lines. The 4-bp deletion is indicated with a box in WT and delTAAT. (D) The *lca5* mRNA levels in 1-month –old wt and *lca5* knockout zebrafish retinas are detected by quantitative PCR. The quantitative data of at least three independent experiments were statistically analyzed using two-tailed Student's *t*-test and shown as mean ± SD.

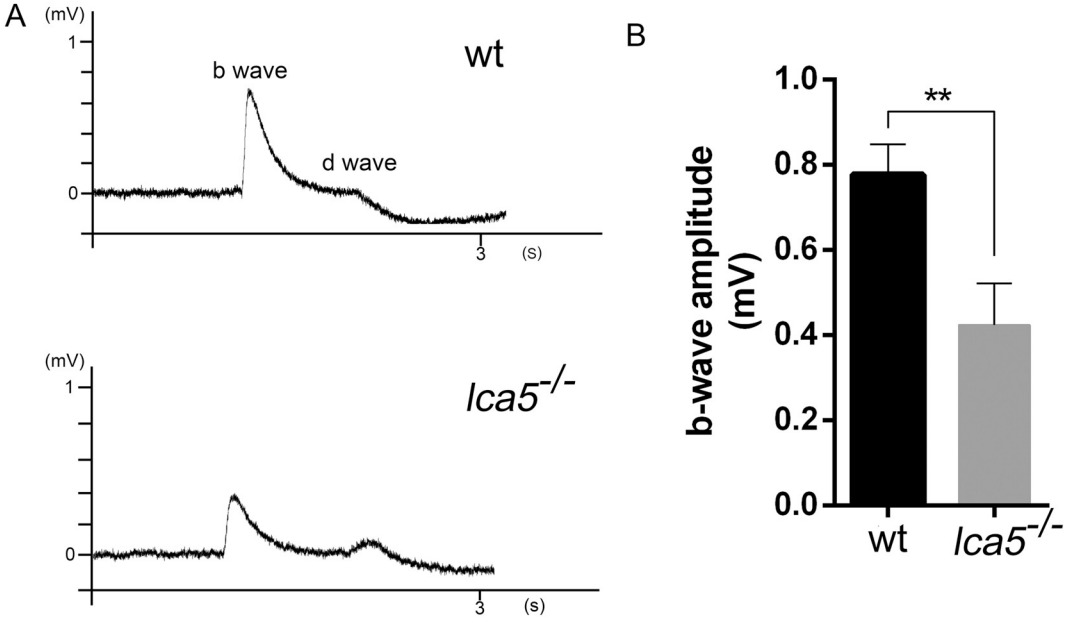

Fig. 2. Visual defect in $lca5^{-/-}$ larval detected by ERG analysis. (A) Representative traces of ERG of wt and *lca5* knockout zebrafish at 7 dpf. (B) Comparison of b-wave amplitudes of wt ($n = 8$) and $lca5^{-/-}$ ($n = 10$) zebrafish using two-tailed Student's *t*-test. The results are shown as mean ± SD. **, $p < 0.01$.

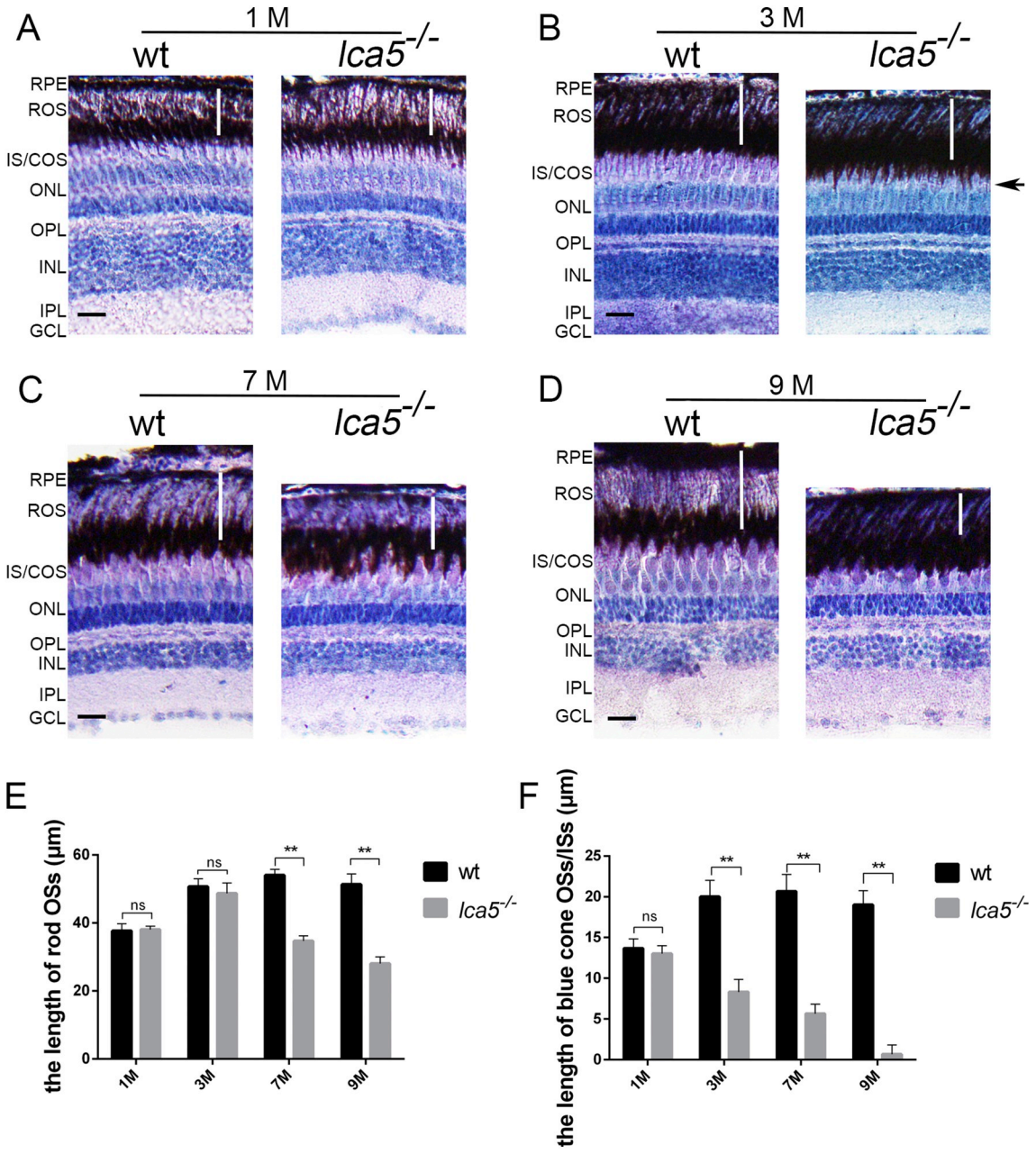

Fig. 3. Progressive degeneration of the outer retina were observed in *lca5* knockout zebrafish. (A–D) Hematoxylin and eosin (H&E) staining analysis of cryosections in wt and *lca5*$^{-/-}$ zebrafish at indicated ages. White lines represent the length of rods outer segments. The black arrow indicates the cones outer segments. RPE, retinal pigment epithelium; ROS, rod outer segment; COS, cone outer segment; IS, inner segment; ONL, outer nuclear layer; OPL, outer plexiform layer; INL, inner nuclear layer; IPL, inner plexiform layer; GCL, ganglion cell layer. Scale bars: 20 μm. (E) Statistical data for the length of rod outer segments. (F) Statistical data for the length of blue cone outer segments/rod inner segments. Three parallel samples were tested for each group, and at least three microscopic fields of each group were quantified and analyzed using two-tailed Student's *t*-test. The results were shown as mean ± SD. **, $p < 0.01$.

knockout retinas at the age of 1 month, 3 months, 7 months and 9 months, respectively. Hematoxylin and eosin (HE) staining was carried out on retinal sections to show the details of retina. In 1-month-old zebrafish, there was no significant difference in retinal structure between wild-type and *lca5* mutants (Fig. 3A). However, at 3 months of age, although the thickness of photoreceptors outer segments of *lca5*$^{-/-}$ zebrafish was similar to that of control, the distance between the photoreceptor outer segment and outer nuclear layer was significantly shorter (Fig. 3B). In zebrafish, photoreceptors are closely arranged in a layered pattern throughout the retina. The outer segment of the blue cone and the inner segment of the rod are in the same layer of the retina [36,37]. As shown by the black arrow in Fig. 3B, this thinning may be due to the degradation of the blue cones outer segments. Furthermore, in 7-month-old *lca5*$^{-/-}$ zebrafish retinas, in addition to the thinning of the inner segment/blue cone outer segment, the photoreceptors outer segments were shortened remarkably, and the outer nuclear layer of photoreceptors was slightly thinner. More specifically, the number of cone nuclei was decreased when compared with wild-type control (Fig. 3C). The phenotype was more pronounced in *lca5* mutants at 9 mouths of age (Fig. 3D). Fig. 3E and F showed the statistical results of the length of the rod OSs and the blue cone OSs/ rod ISs, respectively. These results indicated that *lca5* mutants show progressive photoreceptor degeneration, and the degeneration of cones is more severe than that of rods.

Next, we observed the ultrastructure of the photoreceptor outer segments in wt and *lca5* mutant zebrafish by transmission electron

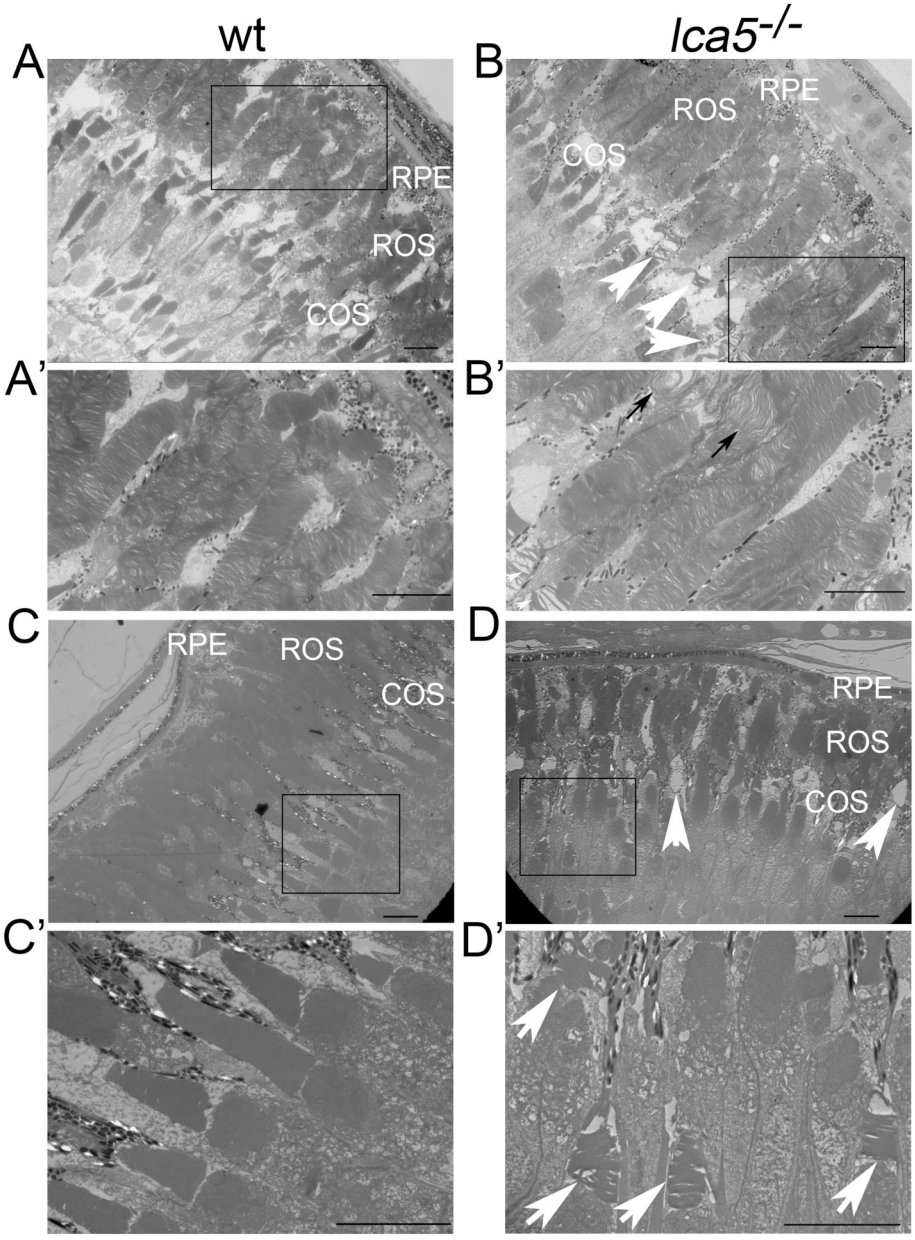

Fig. 4. Ultrastructural analysis of photoreceptors outer segments in wt and *lca5* knockout zebrafish. (A) 21-day-old wt zebrafish retina shows well-maintained photoreceptor outer segments. (A') Enlarged image of the box in (A). (B) 21-day-old *lca5* knockout zebrafish retina exhibits fragmented cone membrane disks and disordered rod outer segment membrane disks. (B') Enlarged image of the box in (B). (C) 3-month-old wt zebrafish retina show complete and ordered retinal structure. (C') Enlarged image of the box in (C). (D) 3-month-old *lca5* knockout zebrafish retina exhibits the disordered and loose retinal structure and the disrupted and disappeared cone outer segment. (D') Enlarged image of the box in (D). White arrow head represents the disrupted and disappeared cone outer segments. Black arrow indicates the disordered rod membrane disks structure. RPE, retinal pigment epithelium; ROS, rod outer segment; COS, cone outer segment. Scale bars: 10 μm.

microscopy. According to the results of HE staining, we selected the time points of 3-week-old and 3-month-old, which are before and after the degeneration of photoreceptor outer segments, respectively. Compared with the wild-type, the 3-week-old *lca5*$^{-/-}$ zebrafish showed no significant difference in the overall structure of the retina (Fig. 4A, B). However, the cone membrane discs were broken into segments and rod membrane discs showed disordered structure (Fig. 4A, B, A', B'), which may be the early stages of progressive degeneration of the photoreceptor outer segments. In 3-month-old zebrafish retina, the overall structure of the retinal photoreceptors, no matter rods or cones, was more disordered and looser than that of wild-type controls (Fig. 4C, D). Furthermore, in 3-month-old *lca5*$^{-/-}$ zebrafish, the cone outer segment membrane discs were disrupted more seriously, and even some cone outer segments disappeared completely (Fig. 4C, D, C', D'). Although there was disordered membrane discs structure in rods in *lca5*$^{-/-}$ zebrafish (Fig. 4A', B', Supplementary Material, Fig. S4), these broken membrane discs similar to cone outer segments were not identified in the rods outer segments, suggesting that the cones are more sensitive than the rods in *lca5*$^{-/-}$ zebrafish. Taken together, our observations demonstrated that the deletion of zebrafish *lca5* leads to progressive photoreceptor degeneration of both rods and cones with cones affected more severely and earlier than rods.

3.4. All four types of cone photoreceptors degenerate earlier than rod photoreceptors

To identify the rod and cone photoreceptors more specifically, we labeled the outer segments of rods and all four types of cones using antibodies against their respective opsins (rhodopsin, opn1lw1, opn1mw1, opn1sw2, opn1sw1). Similar to the results of HE staining, *lca5* knockout zebrafish showed no significant change in the lengths of the rod outer segments at age 3 months compared with wild type (Fig. 5A, B). In 7-month-old *lca5*$^{-/-}$ retinas, the outer segments of rods were shorter than that of wild type control (Fig. 5C). Unlike rods, however, cones degenerated earlier. In 1-month-old *lca5*$^{-/-}$ retinas, the outer segments of the four cones subtypes all showed serious degeneration (Fig. 5D, G, J, M). Furthermore, this phenotype is more pronounced in older *lca5* mutants (Fig. 5E, H, K, N). In 7-month-old zebrafish, the outer segments of the four cones almost disappeared compared to the wild type (Fig. 5F, I, L, O). Statistical results of the

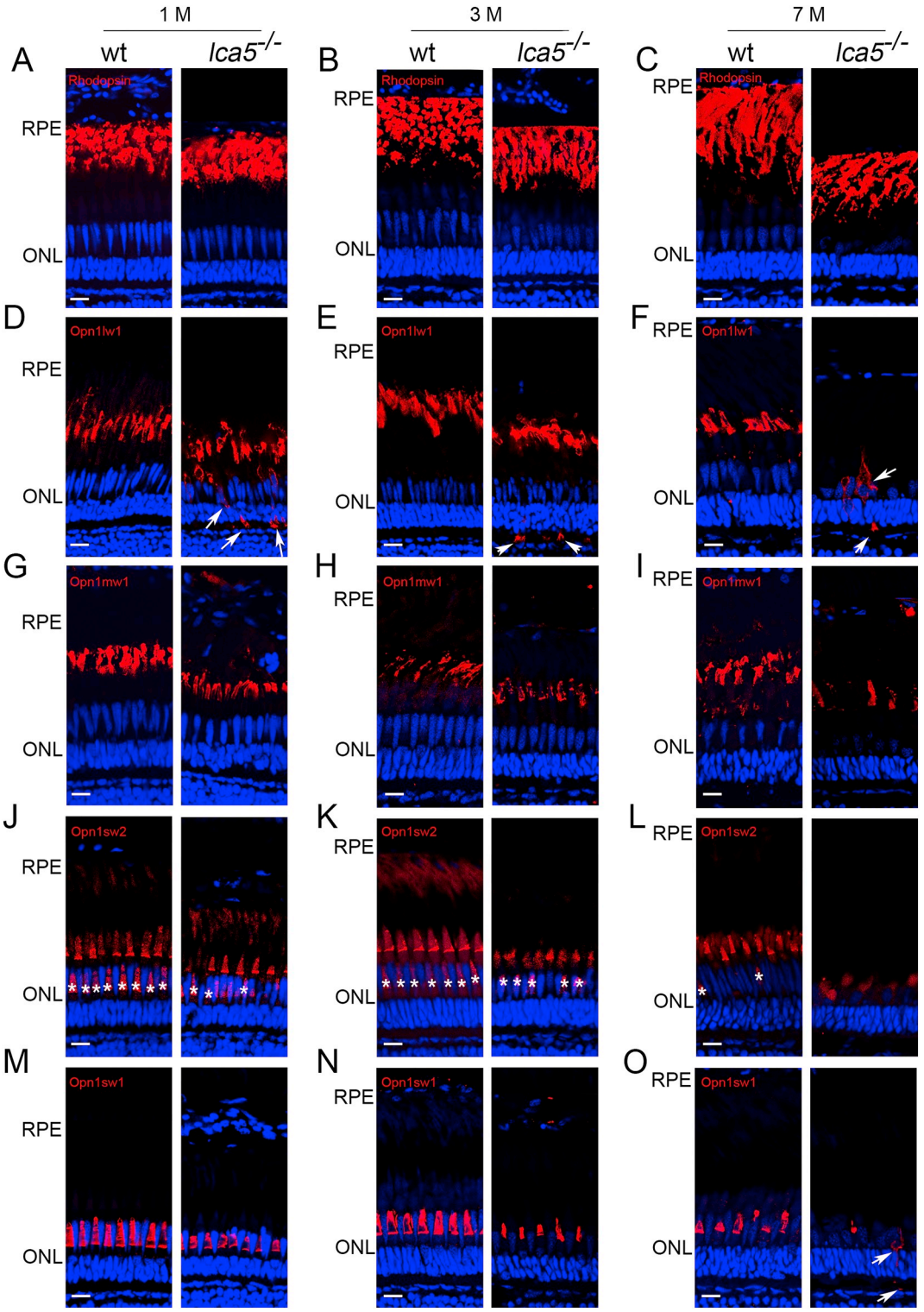

Fig. 5. Progressive photoreceptors degeneration with a predominantly cone-affected pattern in *lca5* knockout zebrafish. (A–C) Retinal cryosections were labeled with rod specific Rhodopsin at indicated ages. (D–O) Retinal cryosections were labeled with cone specific (opn1lw1 for red cones, opn1mw1 for green cones, opn1sw2 for blue cones and opn1sw1 for UV cones) antibodies. White arrows indicates mislocalization of red-cone opsin and UV-cone opsin. White asterisks indicates non-specific staining of blue-cone opsin. Three parallel samples were tested for each group, and at least three microscopic fields of each group were quantified and analyzed. Scale bars: 10 μm.

lengths of the photoreceptor outer segments are shown in supplement material (Supplementary Material, Fig. S5A, B, C, D, E).

In addition, we detected the cone α-transducin (c-Tα,GNAT2) and the rod α-transducin (r-Tα, GNAT1) by western blotting in *lca5*$^{-/-}$ zebrafish at age of 15 days and 2 months (Supplementary Material, Fig. S6A, B). Consistent with our previous observation of photoreceptors degeneration by immunofluorescence, compared with the wild-type zebrafish, the protein level of c-Tα was significantly down-regulated in 2-month-old *lca5* knockout zebrafish, but there was no such change in 15-day-old zebrafish, indicating that the cone outer segment have

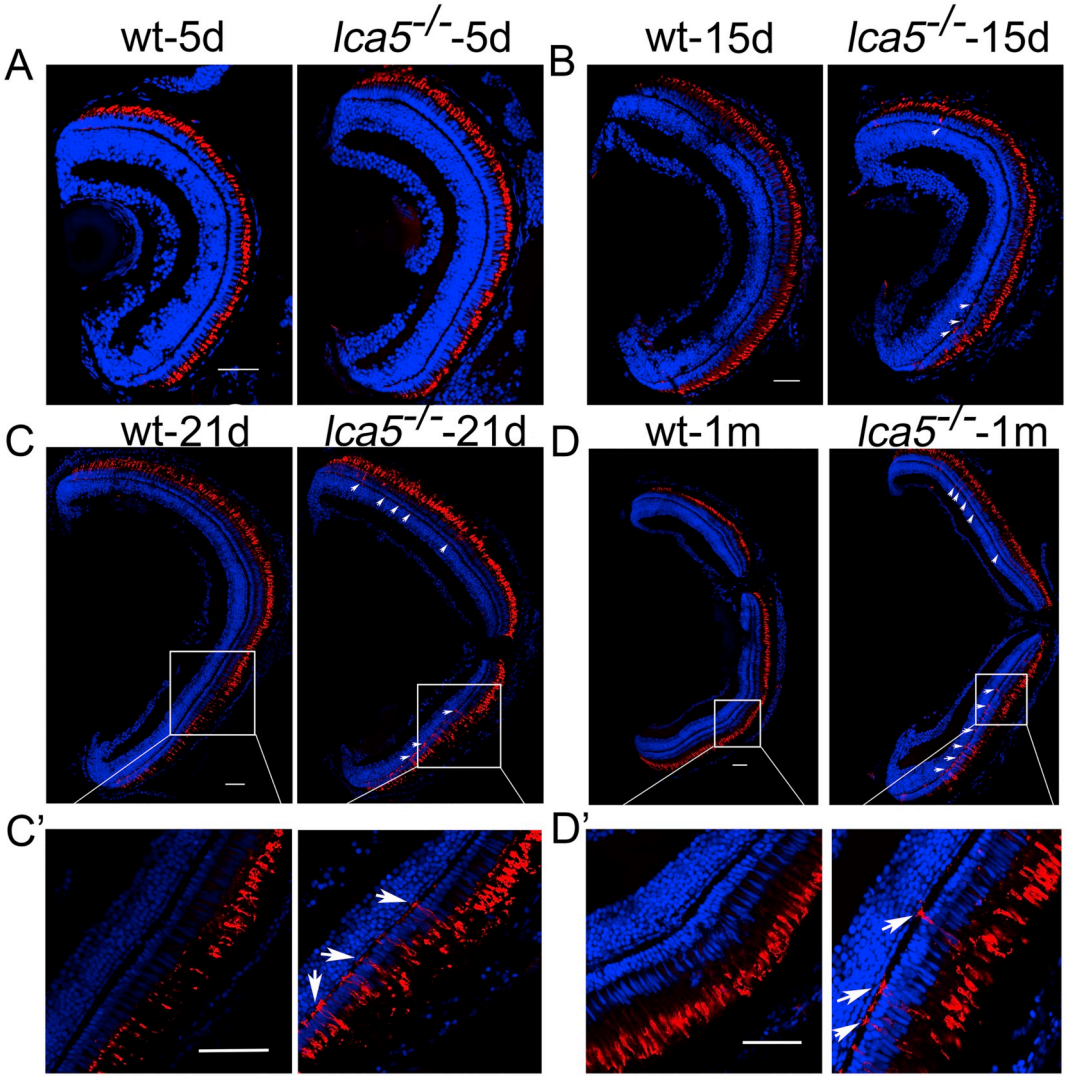

Fig. 6. The mislocalization of red-cone opsin is extended from the peripheral retina to the intermediate retina. (A) Retinal cryosections were labeled with red-cone opsin antibody at 5 dpf, (B) at 15 dpf, (C) at 21 dpf, (D) at 1 mpf. (C') Enlarged image of the box in (C). (D') Enlarged image of the box in (D). White arrows represent the mislocalization of red-cone opsin. Three parallel samples were tested for each group, and at least three microscopic fields of each group were quantified and analyzed. Scale bars: 40 μm.

degenerated in 2-month-old *lca5*$^{-/-}$ zebrafish. However, there was no change in the protein level of r-Tα, suggesting that the rod outer segment have not degenerated at this time.

Together, these results indicated that, compared with the rods, all four types of cones degenerate at an earlier stage in *lca5*$^{-/-}$ zebrafish.

3.5. The impaired outer segment protein trafficking in *lca5*$^{-/-}$ zebrafish

Interestingly, we observed that red-cone opsin mislocated to inner segments, synaptic terminals and outer nuclear layer in the 1-month-old, 3-month-old and 7-month-old *lca5* knockout zebrafish (Fig. 5D, E, F). Similar mislocalization of the UV-cone opsin was found in 7-month-old *lca5*$^{-/-}$ zebrafish retinas, which may be caused by the loss of the UV cone outer segments (Fig. 5O).

To explore when the mislocalization of red cone opsin occur, we examined the *lca5* deficient zebrafish retina by immunostaining since 5 dpf (Fig. 6A, B, C, D). In 5-day-old *lca5* mutants, no abnormality was found in either the length of the red-cone outer segment or the localization of the red-cone opsin compared with the wild-type (Fig. 6A). However, in 15-days-old *lca5* mutants, although there was no obvious degeneration of the red-cone outer segment (Supplementary Material, Fig. S7), we observed mislocalization of red-cone opsins to inner segments, outer nuclear layer and outer plexiform layer (Fig. 6B). Furthermore, these mislocalization occurred in the peripheral region located on the nasal and temporal sides of the zebrafish retina (Fig. 6B). We also detected the green-cone opsin, the blue-cone opsin and the UV-cone opsin by labeling opn1mw1, opn1sw2 and opn1sw1, and found that there was no obvious abnormality in 15-day-old *lca5* knockout zebrafish (Supplementary Material, Fig. S8). In order to understand more fully the process of red-cone opsin mislocalization, we observed 21-day-old and 1-month-old zebrafish retinal slices. In the 21-day-old *lca5*$^{-/-}$ zebrafish retina, the mislocalization of red-cone opsin migrated from the peripheral retinal region to the intermediate retinal region (Fig. 6C, C'). As shown by the white arrowhead in Fig. 6D, the mislocalization phenotype of red-cone opsin was more pronounced in 1-month-old *lca5* knockout zebrafish retina (Fig. 6D, D'). These results demonstrated that the initial mislocalization of red-cone opsin occurs in 15-day-old *lca5* knockout zebrafish, and that the mislocalization is extended from the peripheral retina to the intermediate retina.

In order to investigate which photoreceptor outer segment proteins' trafficking is also affected besides the red-cone opsin in the *lca5* knockout zebrafish, we performed immunofluorescence experiments on

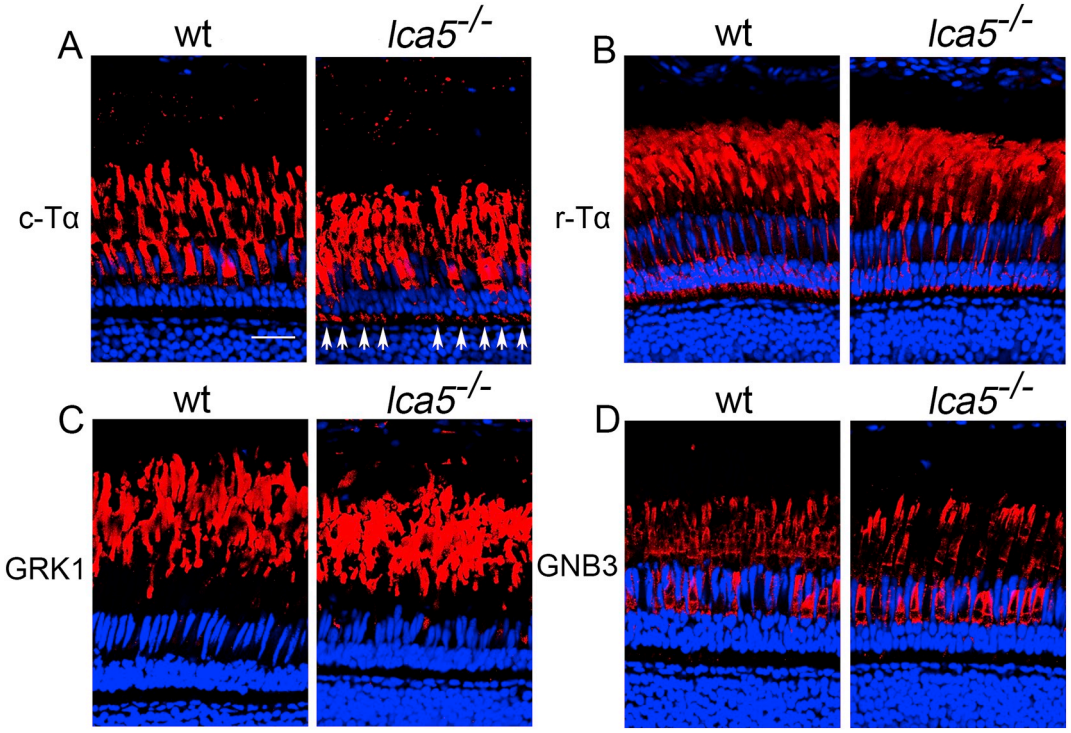

Fig. 7. The retinal localization of c-Tα, r-Tα, GRK1 and GNB3 in 1-month-old wt and *lca5* knockout zebrafish. (A) C-Tα mislocated to inner segment and synaptic terminal. (B–D) No obvious mislocalization of r-Tα, GRK1 and GNB3. White arrows represent the mislocalization of c-Tα. Three parallel samples were tested for each group, and at least three microscopic fields of each group were quantified and analyzed. Scale bars: 10 μm.

1-month-old zebrafish retina using the antibodies recognizing the c-Tα, r-Tα, G-protein-dependent receptor kinase 1 (GRK1) and G-protein beta subunit 3 (GNB3). We found that compared with the wild type, the c-Tα mislocated to inner segment and synaptic terminal in *lca5* knockout zebrafish (Fig. 7A), while r-Tα, GRK1 and GNB3 had no significant mislocalization (Fig. 7B, C, D). These results suggested that Lca5 can selectively participate in the ciliary transport of photoreceptors outer segment proteins.

3.6. Accumulation of Ift88 in the cilia of photoreceptor cells in the *lca5*$^{-/-}$ zebrafish retina

To explore how the *lca5*-deficient zebrafish affects the cilia trafficking of the photoreceptor outer segment proteins, we examined photoreceptor cilia in *lca5*$^{-/-}$ zebrafish retina by immunostaining using antibodies against acetylated α-tubulin and Ift88. In 1-month-old *lca5* knockout zebrafish, there was no significant change in the length of the cilia compared with the wild type (Fig. 8A, C), indicating that ciliary formation was not affected. Furthermore, we found strong accumulation of Ift88 in the photoreceptor cells cilia in *lca5*$^{-/-}$ zebrafish retina, and the Ift88 signal intensity was significantly higher in *lca5*-deficient zebrafish photoreceptor cilia.

In order to confirm that the strong accumulation of Ift88 in the cilia is a cause of photoreceptor outer segment proteins trafficking defects, we studied the 5-day-old zebrafish retina by immunofluorescence (Fig. 8B). In 5-day-old *lca5* knockout zebrafish retina, there was still a large amount of Ift88 in the photoreceptor cilia (Fig. 8B). We also measured the length of photoreceptor cell cilia in 5-day-old *lca5*$^{-/-}$ zebrafish retina, and found no significant difference in the length of the cilia compared with wild type (Fig. 8C). Given that the Ift88 signal intensity was significantly enhanced in the photoreceptor cells cilia in the *lca5* knockout zebrafish, we wondered whether this was caused by the up-regulation of Ift88 protein expression. We detected the Ift88 protein level, but we found no significant up-regulation in the *lca5* knockout zebrafish (Fig. 8D, E). Together, our results indicated that in *lca5* knockout zebrafish, the abnormal distribution of Ift88 in photoreceptor cell cilia may be an important reason for the trafficking defects of photoreceptor outer segment proteins.

In addition, the *lca5* gene mRNA were injected into one-stage *lca5*$^{-/-}$ embryos, and the retinal sections of the 5-day-old zebrafish were detected by immunofluorescence (Supplementary Material, Fig. S9). In the *lca5* knockout zebrafish, Ift88 was distributed throughout the photoreceptor cilia, while in the zebrafish injected with *lca5* mRNA, Ift88 was recruited to the base of the photoreceptor cilia. These results indicated that zebrafish *lca5* gene mRNA could partially rescue the mislocalization of Ift88.

4. Discussion

Leber congenital amaurosis caused by *LCA5* has high clinical heterogeneity, and the patient's retinal phenotype is also different. In LCA patients with *LCA5* mutations, some common clinical symptoms such as an atrophic aspect of the macular area and bone-spicule pigments in the peripheral retina could be observed [15,18,21]. Meanwhile, progressive foveal cone cells loss and night blindness have also been reported in patients with *LCA5* mutations [13,15,38], so it is difficult to determine by phenotypes whether the loss of *LCA5* function is more important for cones or rods, or both. Recently, a cone dystrophy (CD) phenotype caused by *LCA5* pathogenic mutations has been described [22], which may indicate that *LCA5* dysfunction has a more severe effect on cones in that family. Of course, the clinical diversity may be related to the genetic background. In *Lca5* knockout mouse, rhodopsin and red/green cone opsin trafficking are impaired, and the photoreceptor outer segments and inner segments begin to degenerate at an early stage and the photoreceptors disappear completely at 4 months of age. Moreover, it is found that the initiation of photoreceptors outer segments development are delayed and photoreceptors outer segments discs are not oriented properly in *Lca5* knockout mouse [24]. The phenotype of *Lca5* knockout mouse partly explains the pathogenesis of retina in Leber congenital amaurosis patients. Zebrafish is becoming a popular animal

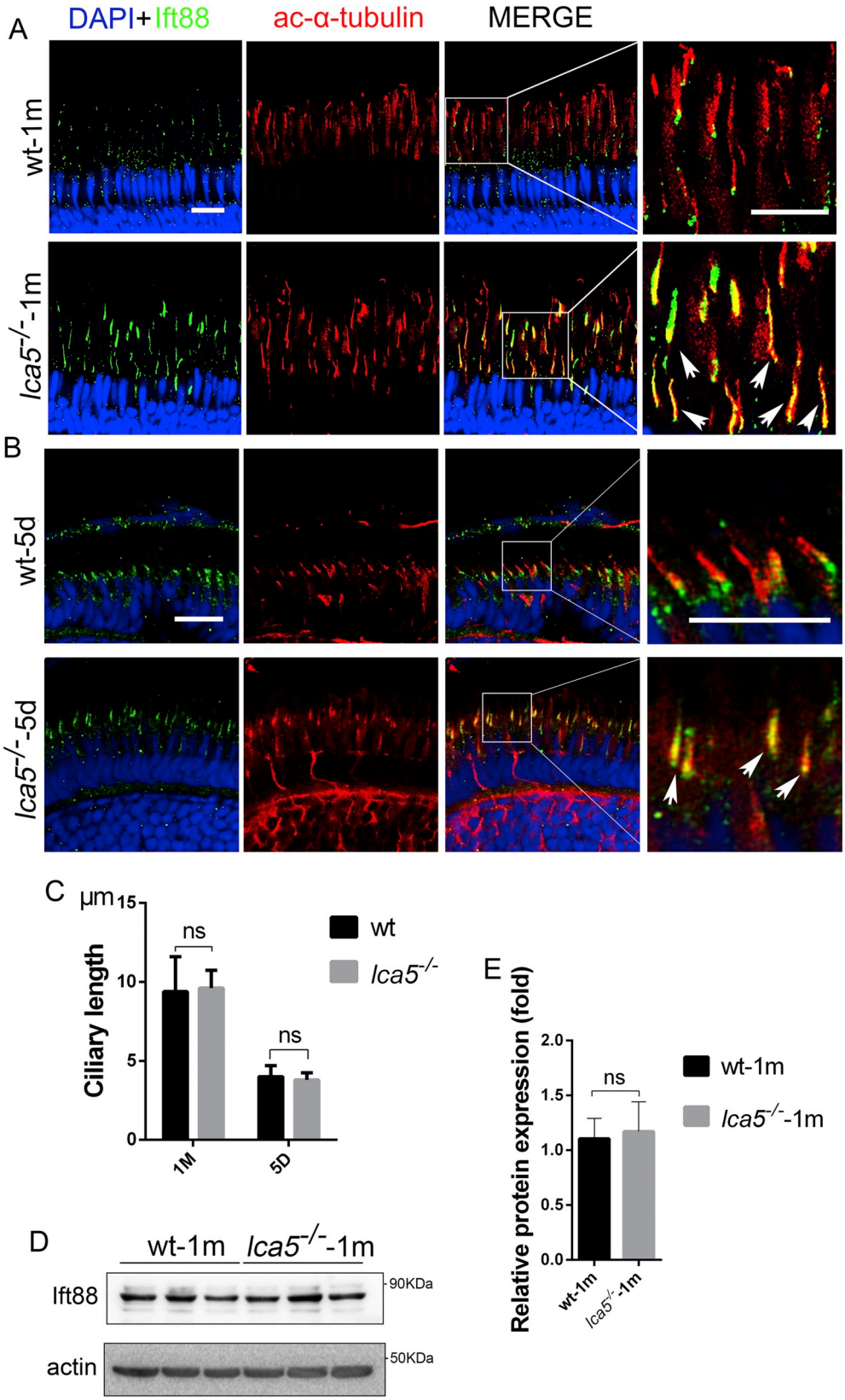

Fig. 8. The strong accumulation of Ift88 in photoreceptor cilia in *lca5*$^{-/-}$ zebrafish retina. (A) The distribution of Ift88 in photoreceptor cilia in 1-month-old wt and *lca5*$^{-/-}$ zebrafish retina. (B) The distribution of Ift88 in photoreceptor cilia in 5-day-old wt and *lca5*$^{-/-}$ zebrafish retina. Scale bars: 10 μm (C) Statistical data for the length of photoreceptor cilia. Three parallel samples were tested, and at least three microscopic fields of each group were quantified and analyzed using two-tailed Student's *t*-test. The results were shown as mean ± SD. ns, no significant. (D) Western blot analysis of Ift88 protein expression levels in 1-month-old wt and *lca5* knockout zebrafish retinas. (E) The quantitative data of at least three independent experiments were statistically analyzed using two-tailed Student's *t*-test and shown as mean ± SD. ns, no significant.

model in genetics and developmental biology. Especially, the retinal structure and the ratio of rods to cones similar to that of human make it an excellent model for studying human retinal diseases [28]. In *lca5* knockout zebrafish, the trafficking of red-cone opsin and c-Tα are impaired, and the degeneration of the cones are more severely affected and earlier than that of rods, leading to a cone-rod dystrophy phenotype. Moreover, the loss of *lca5* function does not seem to affect the early development of photoreceptors, but affects the maintenance of photoreceptor function. Together, in patients with *LCA5* mutations and *lca5* knockout zebrafish, cone damage appears to be more serious, and

the retinal phenotype of *lca5* knockout zebrafish may be more representative of the process of retinopathy in LCA patients.

In the *lca5* knockout zebrafish, the 7-day-old zebrafish ERG response was significantly reduced compared to the wild type, which was consistent with the previously reported phenotype in mouse and humans. In the early stage, the photoreceptors in the zebrafish retina are mainly cones, so rods do not contribute to the ERG of dark-adapted zebrafish until 15 dpf [39,40]. Although we detected abnormal distribution of Ift88 in the photoreceptor cell cilia in the 5-day-old *lca5* knockout zebrafish, we did not detect the red-cone opsin mislocalization and the disordered outer segment in this period. So we speculate that in *lca5*$^{-/-}$ zebrafish retina, there are other important photoreceptor outer segment proteins trafficking affected, and the trafficking defect causes visual defect and leads to the degeneration of the other three types cones outer segment.

The initial mislocalization of red-cone opsin occurs in the peripheral retina of 15-day-old *lca5* knockout zebrafish, and extended to the intermediate retina at 1 mpf. Why does the mislocalization of the red-cone opsin show such a pattern? We speculate that with the continuous expansion of the retina, the newly generated photoreceptors are added at the peripheral retina, making the photoreceptors previously located in the peripheral retina the intermediate retina. Therefore, with the growth of zebrafish retina, the mislocalized photoreceptor outer segment proteins gradually appeared in the intermediate retina and the central retina. Of course, this specific mechanism remains to be further studied.

In *lca5* knockout zebrafish retina, Ift88 is abnormally distributed in the photoreceptor cell cilia. However, in *Lca5* knockout mice, the localization of Ift88 appears to be unaffected [24]. For this question, our understanding is as follows: first, the zebrafish retina differs greatly from the mice retina in both structure and composition [37]. As we previous mentioned, the mice is a rod-dominant retinal structure, and the zebrafish rod-cone ratio is more similar to human; secondly, up to data, the exact function of LCA5 is still unclear. Although LCA5 is conserved from human to zebrafish, the specific functional mechanism of Lca5 in zebrafish and mice may not be identical. As for the abnormal distribution of Ift88 in the photoreceptor cells cilia, we believe that this is a strong accumulation of Ift88 in the cilia caused by the failure of Ift88 to return to the cilia base. In previous reports, there is a direct interaction and co-localization between LCA5 and IFT88 [24], so the trafficking of Ift88 from the cilia top to the cilia base may be affected in the *lca5* knockout zebrafish. In addition, Ift122, a component of IFT complex A, also results in the strong accumulation of Ift88 in photoreceptor cells cilia in *ift122* knockout zebrafish [41]. So the normal trafficking of IFT complex A may be disrupted in the *lca5* knockout zebrafish retina, thus resulting in the abnormal distribution of Ift88 in the photoreceptor cells cilia. This specific mechanism needs to be further studied.

In this study, we generated a *lca5* knockout zebrafish line by CRISPR/Cas9 technology. Early-onset visual defect and progressive photoreceptor cells degeneration were observed. Furthermore, the outer segments degeneration of all four types of cones showed more severely and earlier than that of rods. In *lca5*$^{-/-}$ zebrafish retina, red-cone opsin and c-Tα were selectively mislocalized to inner segment and synaptic terminal. The trafficking defect may be caused by the abnormal distribution of Ift88 in the photoreceptor cilia. Together, our zebrafish model provides a novel platform for functional studies of *LCA5* and identifying potential treatments of LCA in general.

Transparency document

The Transparency document associated with this article can be found, in online version.

Declaration of Competing Interest

The authors declare no conflict of interest.

Acknowledgements

This work was supported by the National Natural Science Foundation of China (No. 81670890, 31571303, 31601026, 31801041 and 81800870).

Appendix A. Supplementary data

Supplementary data to this article can be found online at https://doi.org/10.1016/j.bbadis.2019.07.009.

References

[1] A.I. den Hollander, R. Roepman, R.K. Koenekoop, F.P. Cremers, Leber congenital amaurosis: genes, proteins and disease mechanisms, Prog. Retin. Eye Res. 27 (2008) 391–419.
[2] N. Kumaran, A.T. Moore, R.G. Weleber, M. Michaelides, Leber congenital amaurosis/early-onset severe retinal dystrophy: clinical features, molecular genetics and therapeutic interventions, Br. J. Ophthalmol. 101 (2017) 1147–1154.
[3] J.A. Sahel, Spotlight on childhood blindness, J. Clin. Invest. 121 (2011) 2145–2149.
[4] K. Arcot Sadagopan, R. Battista, R.B. Keep, J.E. Capasso, A.V. Levin, Autosomal-dominant leber congenital amaurosis caused by a heterozygous CRX mutation in a father and son, Ophthalmic Genet. 36 (2015) 156–159.
[5] S.J. Bowne, L.S. Sullivan, S.E. Mortimer, L. Hedstrom, J. Zhu, C.J. Spellicy, A.I. Gire, D. Hughbanks-Wheaton, D.G. Birch, R.A. Lewis, J.R. Heckenlively, S.P. Daiger, Spectrum and frequency of mutations in IMPDH1 associated with autosomal dominant retinitis pigmentosa and leber congenital amaurosis, Invest. Ophthalmol. Vis. Sci. 47 (2006) 34–42.
[6] J.E. Roger, A. Hiriyanna, N. Gotoh, H. Hao, D.F. Cheng, R. Ratnapriya, M.A. Kautzmann, B. Chang, A. Swaroop, OTX2 loss causes rod differentiation defect in CRX-associated congenital blindness, J. Clin. Invest. 124 (2014) 631–643.
[7] R.P. Yadav, N.O. Artemyev, AIPL1: a specialized chaperone for the phototransduction effector, Cell. Signal. 40 (2017) 183–189.
[8] S. Sato, I.V. Peshenko, E.V. Olshevskaya, V.J. Kefalov, A.M. Dizhoor, GUCY2D cone-rod dystrophy-6 is a “phototransduction disease” triggered by abnormal calcium feedback on retinal membrane guanylyl cyclase 1, J. Neurosci. 38 (2018) 2990–3000.
[9] P.M. Amann, K. Czaja, A.V. Bazhin, R. Ruhl, C. Skazik, R. Heise, Y. Marquardt, S.B. Eichmuller, H.F. Merk, J.M. Baron, Knockdown of lecithin retinol acyltransferase increases all-trans retinoic acid levels and restores retinoid sensitivity in malignant melanoma cells, Exp. Dermatol. 23 (2014) 832–837.
[10] F. Pichaud, PAR-complex and crumbs function during photoreceptor morphogenesis and retinal degeneration, Front. Cell. Neurosci. 12 (2018) 90.
[11] R.K. Raghupathy, X. Zhang, F. Liu, R.H. Alhasani, L. Biswas, S. Akhtar, L. Pan, C.B. Moens, W. Li, M. Liu, B.N. Kennedy, X. Shu, Rpgrip1 is required for rod outer segment development and ciliary protein trafficking in zebrafish, Sci. Rep. 7 (2017) 16881.
[12] S. Dharmaraj, Y. Li, J.M. Robitaille, E. Silva, D. Zhu, T.N. Mitchell, L.P. Maltby, A.B. Baffoe-Bonnie, I.H. Maumenee, A novel locus for Leber congenital amaurosis maps to chromosome 6q, Am. J. Hum. Genet. 66 (2000) 319–326.
[13] M.D. Mohamed, N.C. Topping, H. Jafri, Y. Raashed, M.A. McKibbin, C.F. Inglehearn, Progession of phenotype in Leber's congenital amaurosis with a mutation at the LCA5 locus, Br. J. Ophthalmol. 87 (2003) 473–475.
[14] A.I. den Hollander, R.K. Koenekoop, M.D. Mohamed, H.H. Arts, K. Boldt, K.V. Towns, T. Sedmak, M. Beer, K. Nagel-Wolfrum, M. McKibbin, S. Dharmaraj, I. Lopez, L. Ivings, G.A. Williams, K. Springell, C.G. Woods, H. Jafri, Y. Rashid, T.M. Strom, B. van der Zwaag, I. Gosens, F.F. Kersten, E. van Wijk, J.A. Veltman, M.N. Zonneveld, S.E. van Beersum, I.H. Maumenee, U. Wolfrum, M.E. Cheetham, M. Ueffing, F.P. Cremers, C.F. Inglehearn, R. Roepman, Mutations in LCA5, encoding the ciliary protein lebercilin, cause Leber congenital amaurosis, Nat Genet 39 (2007) 889–895.
[15] S. Gerber, S. Hanein, I. Perrault, N. Delphin, N. Aboussair, C. Leowski, J.L. Dufier, O. Roche, A. Munnich, J. Kaplan, J.M. Rozet, Mutations in LCA5 are an uncommon cause of Leber congenital amaurosis (LCA) type II, Hum. Mutat. 28 (2007) 1245.
[16] V.L. Ramprasad, N. Soumittra, D. Nancarrow, P. Sen, M. McKibbin, G.A. Williams, T. Arokiasamy, P. Lakshmipathy, C.F. Inglehearn, G. Kumaramanickavel, Identification of a novel splice-site mutation in the Lebercilin (LCA5) gene causing Leber congenital amaurosis, Mol. Vis. 14 (2008) 481–486.
[17] L. Li, X. Xiao, S. Li, X. Jia, P. Wang, X. Guo, X. Jiao, Q. Zhang, J.F. Hejtmancik, Detection of variants in 15 genes in 87 unrelated Chinese patients with Leber congenital amaurosis, PLoS One 6 (2011) e19458.
[18] A. Ahmad, S. Daud, N. Kakar, G. Nurnberg, P. Nurnberg, M.E. Babar, M. Thoenes, C. Kubisch, J. Ahmad, H.J. Bolz, Identification of a novel LCA5 mutation in a Pakistani family with Leber congenital amaurosis and cataracts, Mol. Vis. 17 (2011) 1940–1945.

[19] M. McKibbin, M. Ali, M.D. Mohamed, A.P. Booth, F. Bishop, B. Pal, K. Springell, Y. Raashid, H. Jafri, C.F. Inglehearn, Genotype-phenotype correlation for leber congenital amaurosis in Northern Pakistan, Arch. Ophthalmol. 128 (2010) 107–113.
[20] D.S. Mackay, A.D. Borman, R. Sui, L.I. van den Born, E.L. Berson, L.A. Ocaka, A.E. Davidson, J.R. Heckenlively, K. Branham, H. Ren, I. Lopez, M. Maria, M. Azam, A. Henkes, E. Blokland, R. Qamar, A.R. Webster, F.P.M. Cremers, A.T. Moore, R.K. Koenekoop, S. Andreasson, E. de Baere, J. Bennett, G.J. Chader, W. Berger, I. Golovleva, J. Greenberg, A.I. den Hollander, C.C.W. Klaver, B.J. Klevering, B. Lorenz, M.N. Preising, R. Ramsear, L. Roberts, R. Roepman, K. Rohrschneider, B. Wissinger, Screening of a large cohort of leber congenital amaurosis and retinitis pigmentosa patients identifies novel LCA5 mutations and new genotype-phenotype correlations, Hum Mutat 34 (2013) 1537–1546.
[21] M. Corton, A. Avila-Fernandez, E. Vallespin, M.I. Lopez-Molina, B. Almoguera, E. Martin-Garrido, S.D. Tatu, M.I. Khan, F. Blanco-Kelly, R. Riveiro-Alvarez, M. Brion, B. Garcia-Sandoval, F.P.M. Cremers, A. Carracedo, C. Ayuso, Involvement of LCA5 in Leber congenital amaurosis and retinitis pigmentosa in the Spanish population, Ophthalmology 121 (2014) 399–407.
[22] X. Chen, X. Sheng, X. Sun, Y. Zhang, C. Jiang, H. Li, S. Ding, Y. Liu, W. Liu, Z. Li, C. Zhao, Next-generation sequencing extends the phenotypic spectrum for LCA5 mutations: novel LCA5 mutations in cone dystrophy, Sci. Rep. 6 (2016) 24357.
[23] A. Beryozkin, L. Zelinger, D. Bandah-Rozenfeld, E. Shevach, A. Harel, T. Storm, M. Sagi, D. Eli, S. Merin, E. Banin, D. Sharon, Identification of mutations causing inherited retinal degenerations in the israeli and palestinian populations using homozygosity mapping, Invest. Ophthalmol. Vis. Sci. 55 (2014) 1149–1160.
[24] K. Boldt, D.A. Mans, J. Won, J. van Reeuwijk, A. Vogt, N. Kinkl, S.J. Letteboer, W.L. Hicks, R.E. Hurd, J.K. Naggert, Y. Texier, A.I. den Hollander, R.K. Koenekoop, J. Bennett, F.P. Cremers, C.J. Gloeckner, P.M. Nishina, R. Roepman, M. Ueffing, Disruption of intraflagellar protein transport in photoreceptor cilia causes Leber congenital amaurosis in humans and mice, J. Clin. Invest. 121 (2011) 2169–2180.
[25] K.L. Coene, R. Roepman, D. Doherty, B. Afroze, H.Y. Kroes, S.J. Letteboer, L.H. Ngu, B. Budny, E. van Wijk, N.T. Gorden, M. Azhimi, C. Thauvin-Robinet, J.A. Veltman, M. Boink, T. Kleefstra, F.P. Cremers, H. van Bokhoven, A.P. de Brouwer, OFD1 is mutated in X-linked Joubert syndrome and interacts with LCA5-encoded lebercilin, Am. J. Hum. Genet. 85 (2009) 465–481.
[26] E. van Wijk, F.F. Kersten, A. Kartono, D.A. Mans, K. Brandwijk, S.J. Letteboer, T.A. Peters, T. Marker, X. Yan, C.W. Cremers, F.P. Cremers, U. Wolfrum, R. Roepman, H. Kremer, Usher syndrome and Leber congenital amaurosis are molecularly linked via a novel isoform of the centrosomal ninein-like protein, Hum. Mol. Genet. 18 (2009) 51–64.
[27] G.J. Lieschke, P.D. Currie, Animal models of human disease: zebrafish swim into view, Nat. Rev. Genet. 8 (2007) 353–367.
[28] J. Chhetri, G. Jacobson, N. Gueven, Zebrafish–on the move towards ophthalmological research, Eye (Lond) 28 (2014) 367–380.
[29] Z. Lu, X. Hu, F. Liu, D.C. Soares, X. Liu, S. Yu, M. Gao, S. Han, Y. Qin, C. Li, T. Jiang, D. Luo, A.Y. Guo, Z. Tang, M. Liu, Ablation of EYS in zebrafish causes mislocalisation of outer segment proteins, F-actin disruption and cone-rod dystrophy, Sci. Rep. 7 (2017) 46098.
[30] S. Yu, C. Li, L. Biswas, X. Hu, F. Liu, J. Reilly, X. Liu, Y. Liu, Y. Huang, Z. Lu, S. Han, L. Wang, J. Yu Liu, T. Jiang, X. Shu, F. Wong, Z. Tang, M. Liu, CERKL gene knockout disturbs photoreceptor outer segment phagocytosis and causes rod-cone dystrophy in zebrafish, Hum. Mol. Genet. 26 (2017) 2335–2345.
[31] F. Liu, J. Chen, S. Yu, R.K. Raghupathy, X. Liu, Y. Qin, C. Li, M. Huang, S. Liao, J. Wang, J. Zou, X. Shu, Z. Tang, M. Liu, Knockout of RP2 decreases GRK1 and rod transducin subunits and leads to photoreceptor degeneration in zebrafish, Hum. Mol. Genet. 24 (2015) 4648–4659.
[32] S. Xie, S. Han, Z. Qu, F. Liu, J. Li, S. Yu, J. Reilly, J. Tu, X. Liu, Z. Lu, X. Hu, T.A. Yimer, Y. Qin, Y. Huang, Y. Lv, T. Jiang, X. Shu, Z. Tang, H. Jia, F. Wong, M. Liu, Knockout of Nr2e3 prevents rod photoreceptor differentiation and leads to selective L-/M-cone photoreceptor degeneration in zebrafish, Biochim. Biophys. Acta Mol. basis Dis. 1865 (2019) 1273–1283.
[33] J.S. Papadopoulos, R. Agarwala, COBALT: constraint-based alignment tool for multiple protein sequences, Bioinformatics 23 (2007) 1073–1079.
[34] Y.V. Makhankov, O. Rinner, S.C. Neuhauss, An inexpensive device for non-invasive electroretinography in small aquatic vertebrates, J. Neurosci. Methods 135 (2004) 205–210.
[35] A. Avanesov, J. Malicki, Analysis of the retina in the zebrafish model, Methods Cell Biol. 100 (2010) 153–204.
[36] P.A. Raymond, L.K. Barthel, A moving wave patterns the cone photoreceptor mosaic array in the zebrafish retina, Int. J. Dev. Biol. 48 (2004) 935–945.
[37] K. Viets, K. Eldred, R.J. Johnston Jr., Mechanisms of photoreceptor patterning in vertebrates and invertebrates, Trends Genet. 32 (2016) 638–659.
[38] S.G. Jacobson, T.S. Aleman, A.V. Cideciyan, A. Sumaroka, S.B. Schwartz, E.A. Windsor, M. Swider, W. Herrera, E.M. Stone, Leber congenital amaurosis caused by Lebercilin (LCA5) mutation: retained photoreceptors adjacent to retinal disorganization, Mol. Vis. 15 (2009) 1098–1106.
[39] C. Crespo, E. Knust, Characterisation of maturation of photoreceptor cell subtypes during zebrafish retinal development, Biol Open, 7, (2018).
[40] J. Bilotta, S. Saszik, S.E. Sutherland, Rod contributions to the electroretinogram of the dark-adapted developing zebrafish, Dev. Dyn. 222 (2001) 564–570.
[41] M. Boubakri, T. Chaya, H. Hirata, N. Kajimura, R. Kuwahara, A. Ueno, J. Malicki, T. Furukawa, Y. Omori, Loss of ift122, a retrograde Intraflagellar transport (IFT) complex component, Leads to slow, progressive photoreceptor degeneration due to inefficient opsin transport, J Biol Chem 291 (2016) 24465–24474.